

Investigation on the partial oxidation of methane to syngas in a tubular $\text{Ba}_{0.5}\text{Sr}_{0.5}\text{Co}_{0.8}\text{Fe}_{0.2}\text{O}_{3-\delta}$ membrane reactor

Haihui Wang, You Cong, Weishen Yang*

State Key Laboratory of Catalysis, Dalian Institute of Chemical Physics, Chinese Academy of Sciences, Dalian 116023, China

Abstract

A perovskite material of $\text{Ba}_{0.5}\text{Sr}_{0.5}\text{Co}_{0.8}\text{Fe}_{0.2}\text{O}_{3-\delta}$ (BSCF), with both electronic and ionic conductivity, was synthesized by a combined citrate–EDTA complexing method. The dense membrane tube made of BSCF was fabricated using the plastic extrusion method. The partial oxidation of methane (POM) to syngas was performed in the tubular BSCF membrane reactor packed with a $\text{LiLaNiO}/\gamma\text{-Al}_2\text{O}_3$ catalyst. The reaction performance of the membrane reactor was investigated as functions of temperature, air flow rate in the shell side and methane concentration in the tube side. The mechanism of POM in the membrane reactor was discussed in detail. It was found that in the tubular membrane reactor, combustion reaction of methane with permeated oxygen took place in the reaction zone close to the surface of the membrane, then followed by steam and CO_2 reforming of methane in the middle zone of the tube side. The membrane tube can be operated steadily for 500 h in pure methane with 94% methane conversion and higher than 95% CO selectivity, and higher than $8.0 \text{ ml/cm}^2 \text{ min}$ oxygen permeation flux.

© 2003 Elsevier B.V. All rights reserved.

Keywords: Ceramic membrane reactor; Perovskite; Methane; POM; Syngas

1. Introduction

The conversion of methane to syngas ($\text{CO} + \text{H}_2$) is an attractive route for the conversion of the large reserves of natural gas [1,2], from which a wide variety of valuable hydrocarbons and oxygenates can be synthesized. Up to now, steam reforming is the dominant process for producing syngas [3]. However, to this process, there are some drawbacks, for example, this reaction is highly energy intensive and also suffers from limitations like poor selectivity for CO and high H_2/CO production ratio, unsuitable for the Fisher-Tropsch synthesis. Large research efforts are

recently being focused on the catalytic partial oxidation of methane (POM) to syngas [4,5].

To date, different kinds of catalysts for POM to syngas with high CO and H_2 selectivity and high CH_4 conversion have been investigated [6–8]. Although the POM with air as the oxygen source is a potential alternative to the steam-reforming process, however, downstream process requirements cannot tolerate nitrogen. Therefore, pure oxygen is required, and the most significant cost associated with conventional POM to syngas is that of the oxygen separation plant.

Dense mixed-conducting oxygen-permeable membranes offer potential solution to several problems in methane conversion [9–17]. This kind of membrane is selectively permeable to oxygen at high temperature, but not to nitrogen or any other gases. Thus, only oxygen from air can be transported through the membrane to the inside of the reactor, where it reacts with

* Corresponding author. Tel.: +86-411-4379073;
fax: +86-411-4694447.
E-mail address: yangws@dicp.ac.cn (W. Yang).
URL: <http://www.yanggroup.dicp.ac.cn>.

the methane, at the same time electrons can transport back to the oxygen-reduction side. As such, there is no external electrodes are needed and cheaper air can be used as oxygen source for POM. Moreover, the hot point producing in the conventional reactor can be eliminated due to the gradual feeding of oxygen through the membrane.

Tsai et al. [14] studied the direct conversion of methane to syngas in a disk-type membrane reactor based on $\text{La}_{0.2}\text{Ba}_{0.8}\text{Co}_{0.2}\text{Fe}_{0.8}\text{O}_{3-\delta}$ at 1123 K. They found that packing a 5% $\text{Ni}/\text{Al}_2\text{O}_3$ catalyst directly on the membrane surface result in a fivefold increase in oxygen permeation flux and fourfold increase in CH_4 conversion, compared with the blank run. Our group [16,17] investigated POM to syngas using a $\text{LiLaNiO}/\gamma\text{-Al}_2\text{O}_3$ as catalyst in a disk-type $\text{Ba}_{0.5}\text{Sr}_{0.5}\text{Co}_{0.8}\text{Fe}_{0.2}\text{O}_{3-\delta}$ (BSCF) membrane reactor. At 1123 K, CH_4 conversion was higher than 98% with the CO selectivity higher than 93%, the oxygen permeation flux reaches $10\text{ ml}/\text{cm}^2\text{ min}$, and the membrane reactor can be operated steadily for 500 h. However, the disk-type membrane has a disadvantage of lower ratio of the reaction area to the volume, as illustrated in literatures [16,18,19]. In such a configuration, a large portion of the methane passing through the reactor may not participate in the reactions, resulting in a lower production efficiency of the methane observed, thereby it is necessary to increase the ratio of area to volume. The tubular membrane has larger ratio of reaction area to volume than the disk-type membrane, so the problem can be partially solved by using tubular membranes with a smaller diameter.

Two methods have been employed to prepare the membrane tube, one is the isostatic pressing method and the other is the plastic extrusion method. Balachandran et al. [12,20,21] and Ma and coworkers [22,23] have reported the results on the tubular oxygen-permeable membrane by the plastic extrusion method. Compared to the isostatic pressing method, the plastic extrusion method can prepare membranes with different shapes and different dimensions. Moreover, the plastic extrusion method can also produce the membrane tube in batches. Therefore, the plastic extrusion method was used to prepare a ceramic membrane tube in this paper. The membrane based on perovskite-type BSCF was chosen in this work due to its high oxygen permeation flux and good structure and chemical stability reported in our previous study

[24]. The purpose of this study is to investigate the syngas production and membrane stability for POM to syngas in the tubular membrane reactor packed with a $\text{LiLaNiO}/\gamma\text{-Al}_2\text{O}_3$ catalyst.

2. Experimental

2.1. Preparation of the dense membrane tube

The BSCF oxide powder was prepared by a combined citrate and EDTA complexing method. Detail information for the preparation of BSCF oxide powder can be found in Ref. [24]. The membrane tube was prepared by extrusion method [25]. The extruded tube was heated at a rate of $5^\circ\text{C}/\text{h}$ in the temperature range of $100\text{--}450^\circ\text{C}$ to facilitate the removal of the gaseous species formed during decomposition of the organic additives, then the heating rate was increased to $1^\circ\text{C}/\text{min}$ and the tube was sintered at $1100\text{--}1200^\circ\text{C}$ in stagnant air for 3–5 h, then the tube was cooled to room temperature with the cooling rate of $2^\circ\text{C}/\text{min}$. The sintered membrane tube had an outer diameter of about 8 mm and an inner diameter of about 5 mm, and length up to 30 cm.

2.2. Membrane reactor setup

A shell and tube reactor was used in this work for the conversion of methane to syngas. The configuration is shown in Fig. 1. The membrane tube served as the tube side of the membrane reactor. Two quartz tubes ($\Phi = 17\text{ mm}$) with grooves at their ends supported the membrane tube with a ceramic binder to seal both ends of the membrane tube into the grooves. Another quartz tube ($\Phi = 29\text{ mm}$) served as the shell side of the membrane reactor. The catalyst was packed in the tube side of the membrane reactor. The heated zone was about 40 cm and the isothermal zone was 10 cm, where the membrane tube was placed. The temperature was measured by a K-type thermocouple encased near the membrane tube. A microprocessor temperature controller (Model AI-708) was used to control the temperatures within $\pm 1\text{ K}$ of the set points. Methane mixed with helium (or pure methane) was fed to the tube side, while air was fed to the shell side. The flow rate of inlet gas was controlled with mass flow controller (model D07-7A/ZM). Both the shell

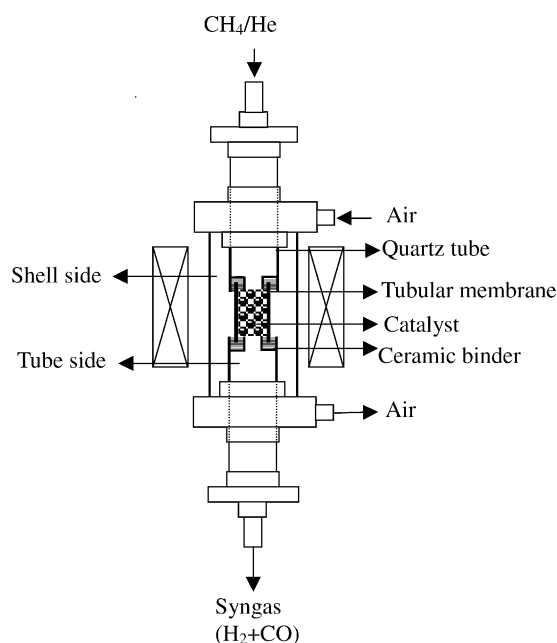


Fig. 1. The schematic of tubular membrane reactor module.

side and the tube side of the reactor were maintained at atmospheric pressure. The products were analyzed by an online gas chromatograph (GC, HP6890 equipped two auto valves) with a porapakQ column and a 13X column. The porapakQ column was used to separate CH_4 and CO_2 , and the 13X column was used to separate H_2 , N_2 , O_2 , and CO . Concentrations of CH_4 , CO_2 , CO , N_2 , O_2 were computed by calibrating against a standard gas mixture containing all the product species in the known quantities. The amount of hydrogen was calculated based on the downstream flow rate. The quantity of H_2O was accounted based on hydrogen atom balance. The oxygen permeation flux was calculated based on oxygen atom balance of all the oxygen-containing products. The conversion of CH_4 , selectivity of CO and H_2 , and the oxygen permeation flux were defined respectively as follows:

$$\text{CH}_4 \text{ conversion} = \frac{F_{\text{CO}_2} + F_{\text{CO}}}{F_{\text{CH}_4}^{\text{outlet}} + F_{\text{CO}_2} + F_{\text{CO}}} \quad (1)$$

$$\text{CO selectivity} = \frac{F_{\text{CO}}}{F_{\text{CO}} + F_{\text{CO}_2}} \quad (2)$$

$$\text{H}_2 \text{ selectivity} = \frac{F_{\text{H}_2}}{F_{\text{H}_2} + F_{\text{H}_2\text{O}}} \quad (3)$$

$$F_{\text{O}_2} = \frac{1}{2}(F_{\text{CO}} + F_{\text{H}_2\text{O}}) + F_{\text{CO}_2} \quad (4)$$

$$J_{\text{O}_2} = \frac{F_{\text{O}_2}}{S} \quad (5)$$

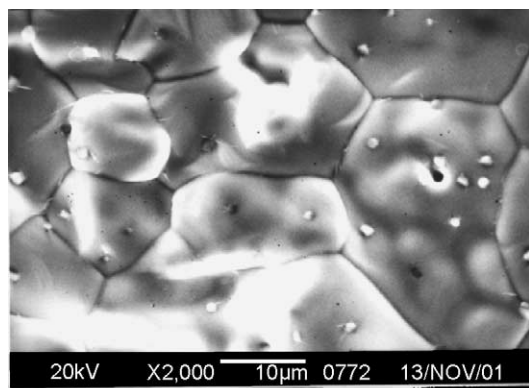
where F_i is the flow rate of species i in ml/min, S the membrane area in cm^2 .

$\text{LiLaNiO}/\gamma\text{-Al}_2\text{O}_3$ was used as the catalyst, the preparation procedure has been described previously [26]. In previous experiments [27–29], we obtained a very high CO selectivity (>98%) and methane conversion (>95%) for POM on this catalyst in the co-feed mode for 500 h.

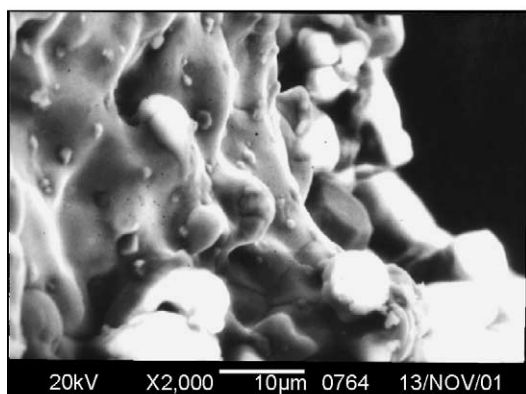
3. Results and discussion

Fig. 2 shows the SEM picture of the fresh membrane tube. For the fresh membrane tube, ceramic grains with clear grain boundaries are visible, and a few of pores can also be seen from the top view of the fresh membrane [Fig. 2(a)]. However, no open pores are found from the across-section of SEM picture, as shown in Fig. 2(b). Moreover, nitrogen permeation measurements confirm that these pores are only closed pores. These closed pores are formed perhaps due to the grain growth or decomposition of organic additives during the sintering of the membrane tube. The density of the sintered membrane tube is determined by Archimedes method with ethanol. Only those membrane tubes having at least 90% relative density are used to construct the membrane reactor for the POM reaction in the following experiments.

After the membrane reactor was sealed at 1040°C , the temperature was lowered to 875°C and air was fed to the shell side. It is necessary to check the leakage before reaction. So pure helium was introduced to the tube side, the leakage through the sealant, if present, can be detected by the nitrogen concentration in the downstream. If leaked oxygen concentration is less than 0.5% of the total oxygen, then the mixture of 80% methane and 20% helium (40.34 ml/min) will be fed to the tube side to replace helium. The effect of air flow rate in the shell side on the reaction performance of POM with the $\text{LiLaNiO}/\gamma\text{-Al}_2\text{O}_3$ in the tubular membrane reactor was investigated. The results are shown in Fig. 3. With the increasing of air flow rate from 200 to 300 ml/min, the conversion of methane increased from 92 to 96%, and the oxygen



(a)



(b)

Fig. 2. SEM pictures of fresh membrane tube: (a) top view; (b) across-section.

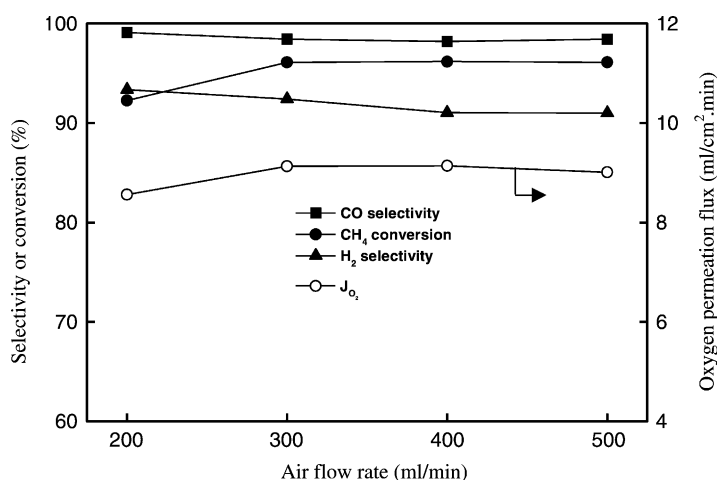


Fig. 3. Effect of air flow rate in the shell side on the membrane reactor performance at 875 °C. Feed (80% CH₄ + 20% He) flow rate is 40.34 ml/min.

permeation flux increased from 8.5 to 9.1 ml/cm² min, while the selectivity of CO and H₂ decreased slightly. These results indicate that the oxygen permeation flux could be influenced by the flow rate of air in the shell side when the flow rate of air is lower than 300 ml/min at 875 °C. However, when the flow rate of air is higher than 300 ml/min, the catalytic performance and oxygen permeation flux reach stable states. These results demonstrate that the external mass transport of oxygen to the membrane surface is not the limiting step for the oxygen permeation when the flow rate of air is higher than 300 ml/min. The similar phenomenon was found in our previous study on the POM in a disk-type oxygen-permeable membrane reactor [17]. In order to eliminate the effect of oxygen external mass transport to the membrane surface, we keep the flow rate of air at 300 ml/min for the further research.

Fig. 4 shows POM performance in the tubular membrane reactor at different temperatures. The flow rate of air in the shell side is 300 ml/min; the flow rate of 80% methane + 20% He in the tube side is 40.34 ml/min. With increasing of temperatures, the CH₄ conversion and the oxygen permeation flux increased, while the selectivity of CO and H₂ decreased. The increase of the oxygen permeation flux is due to the increase of oxygen diffusion rate through the membrane and the surface exchange kinetics with the increase of temperatures.

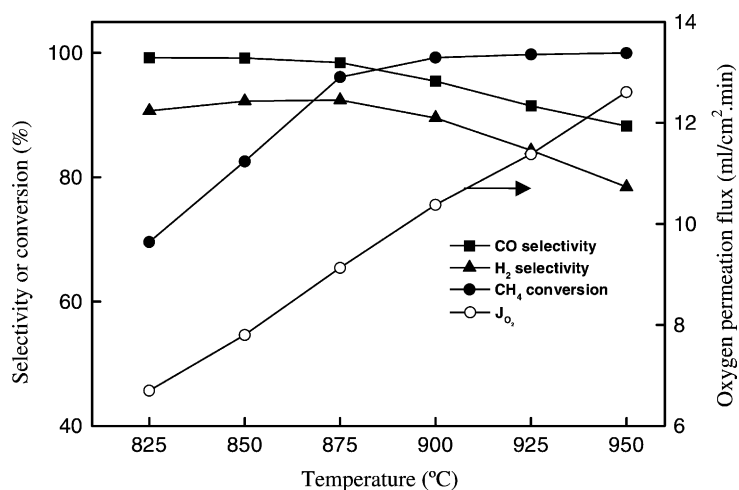


Fig. 4. Effect of temperatures on the membrane reactor performance. The feed (80% CH₄ + 20% He) flow rate is 40.34 ml/min, air flow rate is 300 ml/min.

Fig. 5 compares the oxygen permeation flux under POM reaction condition (CH₄/Air) with that under pure helium condition (He/Air). The feed in the tube side was 80% CH₄ + 20% He or pure He, respectively. The flow rate of the feed was 40.34 ml/min in the both cases. The presence of methane in the tube side can lower the oxygen partial pressure in the tube side deeply, thus enhancing the oxygen permeation flux by a factor of 8–10 times as compared to helium case (He/Air), as shown in Fig. 5, which agrees with the results in disk-type membrane reactor in our group [29].

Fig. 6 shows the dependences of H₂/CO ratio and CH₄/O₂ ratio on the methane concentrations in the tube side. The oxygen permeation flux was calculated based on oxygen atom balance from the oxygen containing products. The results showed that the CH₄/O₂ ratio and the H₂/CO ratio increase with the increase of methane concentration in the tube side. However, the H₂/CO ratio was always lesser than 2 even at the methane concentration was 100% (CH₄/O₂ ratio was 2.2). This result indicates that there is a little carbon deposition takes place on the catalyst because the

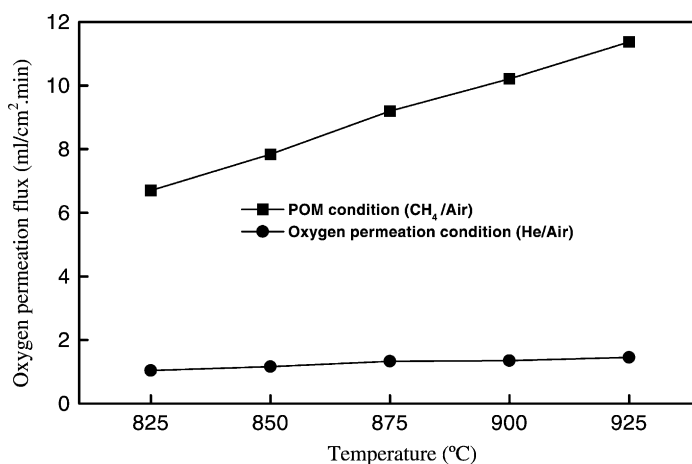


Fig. 5. Comparison of oxygen permeation flux under POM reaction condition (CH₄/air) and under He/air condition. The feed flow rate in the tube side is 40.34 ml/min, air flow rate in the shell side is 300 ml/min.

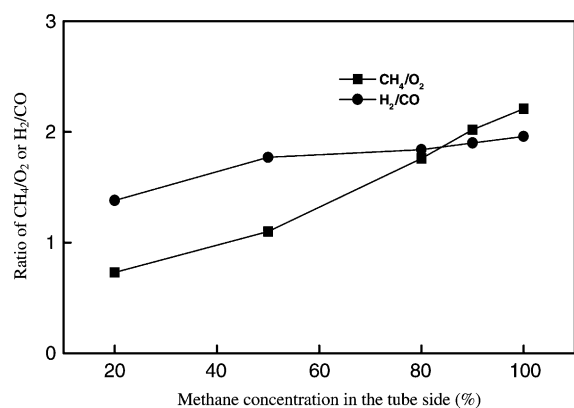


Fig. 6. Effect of methane concentration in the tube side on the ratios of CH₄/O₂ and H₂/CO at 875 °C. The total flow rate in the tube side is 40.34 ml/min, air flow rate in the shell side is 300 ml/min.

H₂/CO ratio should be higher than 2.0 if the carbon deposition on the catalyst is serious. This result also suggests that our membrane reactor and catalyst system can be operated with a little carbon deposition not only at low methane concentration, but also at high methane concentration even in pure methane stream.

Ideal material for the membrane reactor must have sufficient mechanical strength and maintain chemical stability at the desired oxygen permeation flux under the reaction condition. Although, recent reports have described various perovskite-type materials that could be used as ceramic membrane reactors for POM, a few materials can be operated steadily for a long time under the reaction condition. Balachandran et al [12,20,21] investigated POM to syngas by using tubular La_{0.2}Sr_{0.8}Co_{0.2}Fe_{0.8}O_{3-δ} (LSCF) and SrCo_{0.8}Fe_{0.2}O_{3-δ} (SCF) membrane reactors. They found the membranes broke into several pieces within a few minutes after methane was introduced to the membrane reactor at 850 °C. Pei et al. [13] studied the failure mechanism of ceramic membrane reactors on POM to syngas. They observed two types of fractures occurring on the SCF membrane reactor. The first type occurred shortly after the reaction started and the second type often occurred days after the reaction. They also found the first fracture was the consequence of oxygen gradient across the membrane from reaction side to the air side, which causes a little mismatch inside the membrane, leading to fracture;

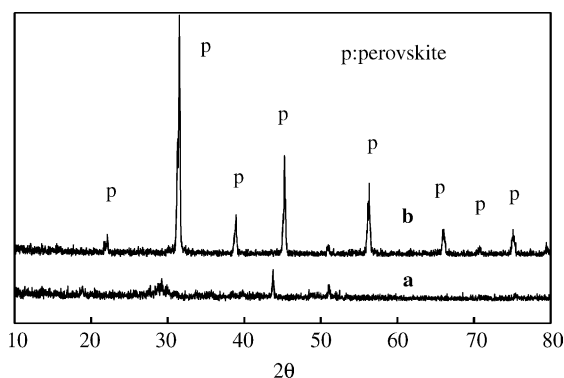


Fig. 7. XRD of (a) treated and (b) untreated sample of BSCF for 1 h in 5% H₂-Ar mixture gas at 900 °C.

the second type of fracture was the result of a chemical decomposition in the reductive atmosphere. It is important to note that no fractures occurring on the BSCF membrane reactor during the POM reaction process. This result indicates the BSCF membrane exhibits better phase stability than the SCF because proper substitution of strontium ion in SCF with barium ion with a larger radius can increase the tolerance factor (near to 1) [24].

The atmosphere in POM reaction is reductive, so it is very important for the membrane reactor to be stable in reductive atmosphere. BSCF sample was treated for 1 h at 900 °C in the 5% H₂-Ar mixture gas, then the sample was quenched to room temperature. The XRD analysis was carried out after the treatment. Fig. 7 shows the XRD patterns of the treated and the untreated samples of BSCF. As shown in Fig. 7, the perovskite structure of the membrane has been completely destroyed in the H₂-containing atmosphere. From the XRD results, the BSCF membrane may be not suitable to be used in membrane reactor for POM to syngas. However, the membrane reactor based on BSCF can be operated for a long time in POM in practical experiment, as shown in Figs. 8 and 9.

Fig. 8 shows CH₄ conversion, CO and H₂ selectivity and oxygen permeation flux after the introduction of a mixture of 80% CH₄ + 20% He at 875 °C in the BSCF tubular membrane reactor. The flow rate of air is 300 ml/min in the shell side and the flow rate of the mixture of 80% methane and 20% He is 40.34 ml/min in the tube side. As shown in Fig. 8, methane conversion was higher than 94%, CO selectivity was 98%

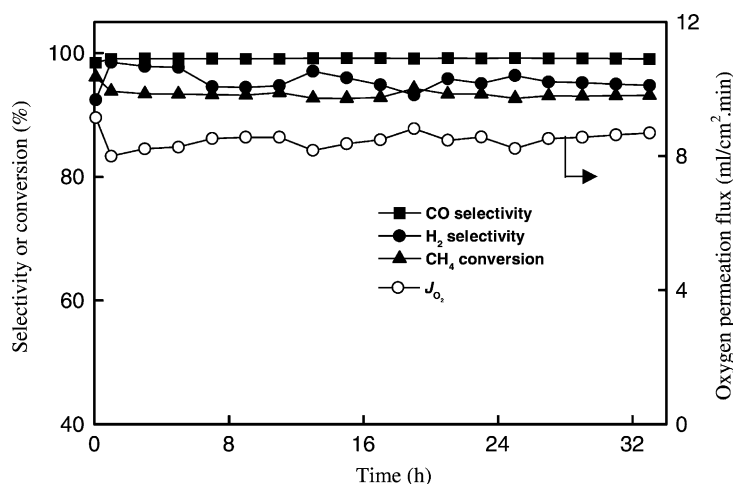


Fig. 8. Methane conversion, CO and H₂ selectivity and oxygen permeation flux in the membrane reactor for POM reaction at 875 °C. The feed (80% CH₄ + 20% He) flow rate in the tube side is 40.34 ml/min, air flow rate in the shell side is 300 ml/min.

and H₂ selectivity was higher than 95%, the oxygen permeation flux was about 8.8 ml/cm² min. The membrane can be operated steadily without any fractures. At 35 h, an abrupt failure of power supplies lead to the ending of the experiment.

Further confirmation of the stability of the membrane tube is shown in Fig. 9. There was a little carbon deposition on the catalyst, when methane concentration was 100% (discussed in Fig. 6), so the pure

methane was used in this time. The flow rate of pure methane in the tube side is 45.28 ml/min; the flow rate of air in the shell side is 300 ml/min. The reaction temperature is 875 °C. During 500 h operation, methane conversion was about 94%, CO selectivity was higher than 95%, and the oxygen permeation flux was higher than 8.0 ml/cm² min. From these results, we can conclude that the BSCF membrane can be operated steadily for a long time in POM reaction,

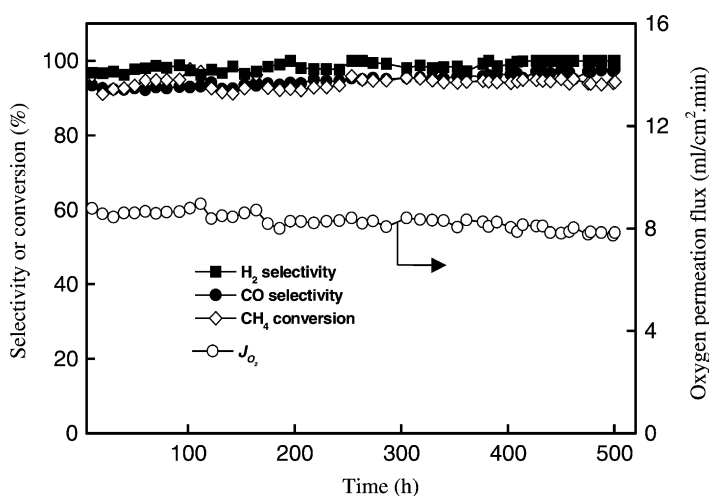


Fig. 9. Long-term performance of reaction in the tubular membrane reactor at 875 °C. The feed (pure methane) flow rate in the tube side is 45.28 ml/min, the flow rate of air in the shell side is 300 ml/min.

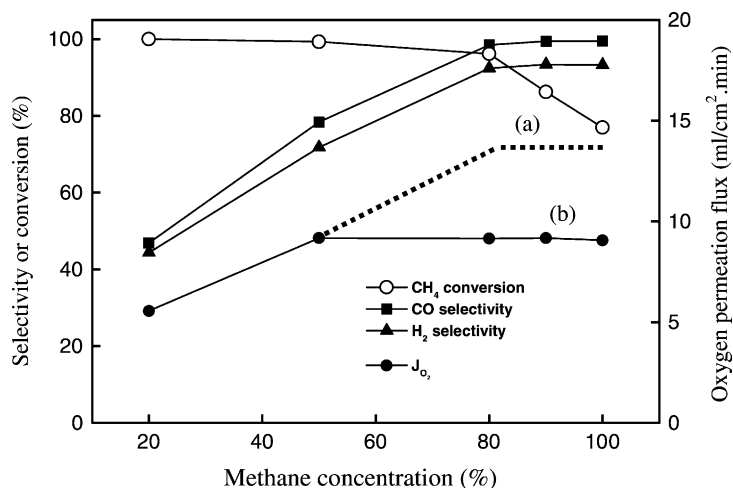


Fig. 10. Effect of the methane concentrations in the tube side on the membrane reactor performance at 875 °C. The total flow rate in the tube side is 40 ml/min, air flow rate in the shell side is 300 ml/min.

which is contrary to the XRD results. Why can the BSCF membrane reactor be operated steadily for a long time for POM reaction? One reason discussed in our previous paper [30] for disk-type membrane reactor is that BSCF membrane has a good structure reversibility, i.e. the surface of BSCF membrane exposed to the reaction atmosphere may be reduced by produced syngas (CO + H₂), however, the reduced layer can be soon re-oxidized by permeated oxygen through the membrane to the original structure. For the tubular membrane reactor, another reason, i.e. mechanism of POM in the tubular membrane reactor, maybe also plays some roles in stabilizing the BSCF membrane structure.

Two main mechanisms of POM to syngas have been proposed in the literatures [4,7]. One is combustion and reforming mechanism (CRR mechanism). The other one is direct partial oxidation mechanism (DPO mechanism). In general, the CRR mechanism takes place at low space velocity (<10⁵ l/kg h) [4], while the DPO mechanism takes place at high space velocity (>10⁵ l/kg h) [7]. The space velocity is around 10⁴ l/kg h in the membrane reactor, the mechanism of POM in the membrane reactor may follow the CRR mechanism.

Fig. 10 shows the influence of methane concentrations in the tube side on the POM performance at 875 °C. The total feed flow rate is 40 ml/min. The

different methane concentrations are obtained by adjusting the ratio of methane to helium. As shown in Fig. 10, with the increase of methane concentrations, methane conversion decreased slightly at first, then decreased sharply when the methane concentrations were higher than 80%. On the contrary, the selectivity of CO and H₂ increased sharply with the increase of methane concentrations at first, then levered off when methane concentrations were higher than 80%. If the POM reaction in the tubular membrane reactor followed the DPO mechanism, the change trend of oxygen permeation flux with the increase of methane concentrations would be same as that of CO selectivity, i.e. the oxygen permeation flux would sharply increase with the increase of methane concentration until 80%, shown in Fig. 10 (line a). However, the oxygen permeation flux increased only at methane concentration lower than 50%, then levered off, as shown in Fig. 10 (line b). This phenomenon suggests that POM reaction in the tubular membrane reactor follows the CRR mechanism, i.e. all the permeated oxygen is used up by the complete combustion of methane ($\text{CH}_4 + 2\text{O}_2 = \text{CO}_2 + 2\text{H}_2\text{O}$), subsequently, the residual methane is reformed by steam ($\text{CH}_4 + \text{H}_2\text{O} = \text{CO} + 3\text{H}_2$) and carbon dioxide ($\text{CH}_4 + \text{CO}_2 = 2\text{CO} + 2\text{H}_2$) to form syngas. As we known, the oxygen permeation flux depends on the oxygen gradient across the membrane. When the methane concentration was

higher than 50%, the increased methane react only with CO_2 and H_2O produced by methane combustion to form syngas rather than directly react with O_2 . So the oxygen partial pressure near the membrane surface would keep unchanged with the increase of the methane concentration, which results in the oxygen permeation flux levered off at the methane concentration increased from 50 to 100%. Under reaction conditions, the oxygen permeation flux was $9.1 \text{ ml/cm}^2 \text{ min}$ and the membrane area was about 2.0 cm^2 , so the total oxygen amount is about 18.2 ml/min . In order to consume all the permeated oxygen, at least 9.1 ml/min methane should be fed to the membrane tube side based on the combustion reaction: $\text{CH}_4 + 2\text{O}_2 = \text{CO}_2 + 2\text{H}_2\text{O}$. Otherwise, some of the oxygen permeated could not be consumed, which would result in the increase of partial oxygen pressure near the surface of the membrane in the tube side and led to the decrease of oxygen permeation flux. When the methane concentration is 20%, the amount of methane is only 8.07 ml/min , which cannot consume up all the permeated oxygen and result in the increase of oxygen partial pressure in the tube side. So the oxygen permeation flux is only $5.6 \text{ ml/cm}^2 \text{ min}$ at methane concentration of 20%, much lower than $9.1 \text{ ml/cm}^2 \text{ min}$ at methane concentration of 50%.

The CRR mechanism of POM in the tubular membrane reactor can also be confirmed by the catalyst distribution after POM reaction. Helium instead of air and methane was fed to both shell side and tube side of the membrane reactor after the POM experiments. The membrane reactor was rapidly cooled down to room temperature under the inert gas atmosphere. It was found that the catalyst consists three layers along the radial direction, i.e. the blue layer, the gray layer, and the black layer, as shown in Fig. 11. The very thin blue layer was closed to the inner surface of the

membrane. The color was similar to the fresh catalyst, which is NiAl_2O_4 . In our previous study on the POM in a disk membrane reactor based on BSCF, the same phenomenon was observed [17]. NiO was detected in the gray layer and Ni^0 was found in the black layer based on the XRD. Lunsford and coworkers [4] investigated POM to syngas over a $\text{Ni/Al}_2\text{O}_3$ catalyst. They also observed that the catalyst bed consists of three different regions. The first region is NiAl_2O_4 , which has only moderate activity for complete oxidation of methane to CO_2 and H_2O . The second region is $\text{NiO} + \text{Al}_2\text{O}_3$, on which the complete oxidation of methane to CO_2 and H_2O occurs. The third region consists of reduced $\text{Ni}^0/\text{Al}_2\text{O}_3$ phase, where reforming reactions of CH_4 with CO_2 and H_2O take place.

According to the reaction phenomenon and the state of the catalyst after POM reaction, the mechanism of POM in the tubular membrane reactor may follow the CRR mechanism. In the tubular membrane reactor, the combustion of methane, $\text{CH}_4 + 2\text{O}_2 = \text{CO}_2 + 2\text{H}_2\text{O}$, with all the permeated oxygen firstly take place on NiAl_2O_4 and $\text{Ni/Al}_2\text{O}_3$ in the reaction zone near the inner surface of the membrane tube, then the reforming reaction of the residual methane by H_2O and CO_2 , i.e. $\text{CH}_4 + \text{CO}_2 = 2\text{CO} + 2\text{H}_2$, $\text{CH}_4 + \text{H}_2\text{O} = \text{CO} + 3\text{H}_2$, occurs on $\text{Ni}^0/\text{Al}_2\text{O}_3$ in the middle zone of the membrane tube. The different nickel species are responsible for different reactions, so different reactions take place in different regions, as shown in Fig. 11. The combustion reaction ($\text{CH}_4 + 2\text{O}_2 = \text{CO}_2 + 2\text{H}_2\text{O}$) took place in the blue and gray layers, while the reforming reactions ($\text{CH}_4 + \text{CO}_2 = 2\text{CO} + 2\text{H}_2$, $\text{CH}_4 + \text{H}_2\text{O} = \text{CO} + 3\text{H}_2$) took place in the black layer. Therefore, gases directly contacting with the membrane tube wall are CO_2 and H_2O rather than H_2 and CO . CO_2 and H_2O are not reductive gases, so the membrane reactor

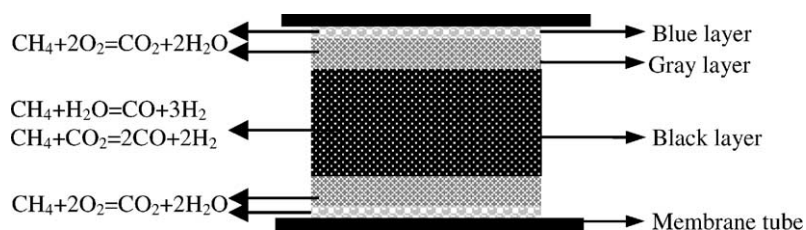


Fig. 11. Schematic representation of $\text{LiLaNiO}/\gamma\text{-Al}_2\text{O}_3$ catalyst bed layers and different reactions in the different regions in membrane tube reactor.

based on BSCF can be operated steadily for long time during the POM reaction.

4. Conclusion

The POM to syngas was investigated in a dense tubular membrane reactor. The membrane tube based on BSCF was made by the plastic extrusion method. The POM performance under different temperatures and methane concentrations were reported. The oxygen permeation flux of the membrane tube in POM was higher than 8.0 ml/cm² min, which is eight times compared to helium case (He/Air). The tubular membrane reactor can be operated steadily for a long time without fractures. During 500 h operation in pure methane at 875 °C, relatively stable oxygen permeation flux was obtained and CO selectivity was higher than 95% with about 94% methane conversion. The mechanism of POM in the membrane reactor is likely the CRR mechanism, which is favor to the stability of the BSCF membrane in POM.

Acknowledgements

The authors gratefully acknowledge financial supports from the Ministry of Science and Technology, China (Grant No. G1999022401) and the National Advanced Materials Committee of China (Grant No. 715-006-0122).

References

- [1] N.D. Spenser, C.J. Pereira, J. Catal. 116 (1989) 399.
- [2] H.D. Gescer, N.R. Hunter, Chem. Rev. 85 (1985) 235.
- [3] J.R. Rostrup-Nielsen, Catal. Today 18 (1993) 305.
- [4] D. Dissanayake, M.P. Rosynek, K.C.C. Kharas, J.H. Lunsford, J. Catal. 132 (1991) 117.
- [5] D.A. Hickman, L.D. Schmidt, Science 259 (1993) 343.
- [6] A.T. Aschcroft, A.K. Cheethan, J.S. Foord, M.L.H. Green, C.P.J. Grey, A. Murrell, P.D.F. Vernon, Nature 344 (1990) 319.
- [7] D.A. Hickman, L.D. Schmidt, AIChE J. 39 (1993) 1164.
- [8] W.J.M. Vermeiren, E. Blomsma, P.A. Jacobs, Catal. Today 13 (1992) 427.
- [9] T. Nozaki, O. Yamazaki, K. Omata, Chem. Eng. Sci. 47 (1992) 2945.
- [10] D. Eng, M. Stoukides, Catal. Rev. Sci. Eng. 33 (1991) 375.
- [11] W. Wang, Y.S. Lin, J. Membr. Sci. 103 (1995) 19.
- [12] U. Balachandran, J.T. Dusek, R.L. Mieville, R.B. Poeppel, M.S. Kleefish, S. Pei, T.P. Kobylinski, J. Faber, C.A. Bose, Appl. Catal. A 133 (1995) 219.
- [13] S. Pei, M.S. Kleefish, T.P. Kobylinski, J. Faber, C.A. Udovich, Z. McCoy, B. Dabrowski, U. Balachandran, R.B. Poeppel, Catal. Lett. 30 (1995) 201.
- [14] C.Y. Tsai, A.G. Dixon, W.R. Moser, Y.H. Ma, AIChE J. 43 (1997) 2741.
- [15] C.Y. Tsai, A.G. Dixon, Y.H. Ma, W.R. Moser, M.R. Pascucci, J. Am. Ceram. Soc. 81 (1998) 1437.
- [16] H. Dong, G.X. Xiong, Z.P. Shao, S.L. Liu, W.S. Yang, Chin. Sci. Bull. 45 (2000) 224.
- [17] H. Dong, Z.P. Shao, G.X. Xiong, J.H. Tong, S.S. Sheng, W.S. Yang, Catal. Today 67 (2001) 3.
- [18] S. Xu, W.J. Thomson, AIChE J. 43 (1997) 2731.
- [19] Y. Zeng, Y.S. Lin, S.L. Swartz, J. Membr. Sci. 150 (1998) 87.
- [20] U. Balachandran, J.T. Dusek, S.M. Sweeney, R.B. Poeppel, R.L. Mieville, P.S. Maiya, M.S. Kleefish, S. Pei, T.P. Kobylinski, C.A. Udovich, C.A. Bose, Ceram. Soc. Bull. 74 (1995) 117.
- [21] U. Balachandran, J.T. Dusek, P.S. Maiya, B. Ma, R.L. Mieville, M.S. Kleefish, C.A. Udovich, Catal. Today 36 (1997) 117.
- [22] Y.P. Lu, A.G. Dixon, W.R. Roser, Y.H. Ma, U. Balachandran, J. Membr. Sci. 170 (2000) 27.
- [23] Y.P. Lu, A.G. Dixon, W.R. Roser, Y.H. Ma, U. Balachandran, Catal. Today 56 (2000) 297.
- [24] Z.P. Shao, H. Dong, G.X. Xiong, Y. Cong, W.S. Yang, J. Membr. Sci. 172 (2001) 177.
- [25] H.H. Wang, Y. Cong, W.S. Yang, J. Membr. Sci. 209 (2002) 143.
- [26] S.L. Liu, G.X. Xiong, W.S. Yang, S.S. Sheng, React. Kinet. Catal. Lett. 68 (2) (1999) 243.
- [27] S.L. Liu, G.X. Xiong, S.S. Sheng, W.S. Yang, Appl. Catal. A 198 (2000) 261.
- [28] S.L. Liu, G.X. Xiong, H. Dong, W.S. Yang, Appl. Catal. A 202 (2000) 141.
- [29] S.L. Liu, G.X. Xiong, H. Dong, W.S. Yang, W. Chu, Z.L. Yu, in: Proceedings of the 12th ICC, Granada Spain, July 9–14, 2000.
- [30] Z.P. Shao, H. Dong, G.X. Xiong, Y. Cong, W.S. Yang, J. Membr. Sci. 183 (2001) 181.